Last-millennium summer-temperature variations in Brianconnais (French Alps) based on a composite tree-ring larch chronology

Christophe Corona, Jean-Louis Édouard, Frédéric Guibal, Lambert Georges Noël, Vanessa Py, Joel Guiot, Thomas André

Last-millennium summer-temperature variations in Brianconnais (French Alps) based on a composite tree-ring larch chronology.

Corona Christophe[1], Edouard Jean-Louis[2], Guibal Frédéric[1], Lambert Georges Noël[3], Py Vanessa[5], Guiot Joël[4], Thomas André[1]

1 - Institut Méditerranéen d'Écologie et de Paléoécologie – Centre National de la Recherche Scientifique (UMR 6116), Université Paul Cézanne, Bâtiment Villemin, Europôle de l'Arbois BP 80, 13545 Aix-en-Provence cedex 4, France.

2 - Centre Camille Julian – Centre National de la Recherche Scientifique (UMR 6572), Maison Méditerranéenne des Sciences de l'Homme, 5 rue du Château de l'Horloge BP 647, 13094 Aix-en-Provence cedex, France.

3 - Université de Franche-Comté – Centre National de la Recherche Scientifique (UMR 6249), Besançon, France.

4 - Centre Europeen de Recherche et d'Enseignement des Géosciences de l'Environnement – Centre National de la Recherche Scientifique UMR 6635 CNRS / Aix-Marseille Université, BP 80, 13545 Aix-en-Provence cedex 4, France.

5 - Laboratoire d'Archéologie Médiévale Méditerranéenne Centre National de la Recherche Scientifique (UMR 6572), Maison Méditerranéenne des Sciences de l'Homme, 5 rue du Château de l'Horloge BP 647, 13094 Aix-en-Provence cedex, France.

Corresponding authors
Christophe Corona: christophe.corona@gmail.com
Jean-Louis Edouard: jean-louis.edouard@mmsh-univ.fr

Résumé

We present a tree-ring-based reconstruction of last millenium summer temperature from Briançonnais in the northern French Alps. The sample material is derived from multi-centennial living trees and also includes larch (Larix decidua Mill.) series from historical construction timbers. The Regional Curve Standardization method was applied to preserve interannual to multicentennial variations in this high-elevation dataset. The proxies are inferred using a linear model and calibrated using the June to August mean temperatures from the last revised version of the HISTALP database spanning the 1760–2003 and adjusted to take into account warm bias before 1850. The transfer function has cross-validated coefficients of correlation (r) of 0.48 (0.42), reductions of error (RE) of 0.21 (0.27) and coefficients of efficiency of 0.20 (0.16). The concordance of the Briançonnais temperature reconstruction with other Alpine records suggests that the transfer function has successfully reconstructed past summer temperature during the last two millennia. Evidence was found of a warm episode between and 900 and 1200AD, and a cold phase between 1500 and 1850AD. These events were possibly correlated to the so-called 'Mediaeval Warm Period' (MWP) and 'Little Ice Age' (LIA). model reconstructed a summer temperature decrease more than 2°C for the LIA compared with the temperature prevailing during the MWP.

Key words: Briançonnais, dendrochronology, *Larix decidua* Mill., construction wood, composite multi-centennial chronologies, climate reconstruction,
Mots clés: Briançonnais, dendrochronologie, *Larix decidua* Mill., bois de construction, chronologies composites pluri-centenaires, reconstruction climatique.

1. Introduction

To date, numerous temperature reconstructions have been produced from local tree-ring chronologies and regional-scale network compilations. However, most of them span the last 300–500 years only. There are relatively few that extend back prior to 1000AD. This lack is very apparent in Jansen et al. (2007), which shows only 16 locations globally from which tree-ring data have been used in millennium long temperature reconstructions. It is related to the scarcity of wood material from the early part of the last millennium and it limits the assessment of climate variations during the putative

Medieval Warm Period (MWP) (Lamb,1977). These difficulties may be overcome by combining data from living trees with those from dry dead and sub-fossil wood (Nicolussi and Schiebling, 2002) together with dendroarchaeological sources. This is done for the Briançonnais region (French Alps) using living trees and historical samples from elevations sites >1,500 m asl, where summer temperature is the main limiting factor for many Alpine tree species (Frank and Esper, 2005). The resulting composite chronologies cover the past 1250 years and allow the assessment of long-term temperature trends for the region especially during the MWP and the Little Ice Age (LIA, e.g. Grove, 1988). In Sect. 2.1, the compiled dataset from living trees and historical timber is introduced. Individual ring width measurements are standardized using the regional curve standardization method (RCS, e.g. Briffa et al., 1992), which may help to preserve long-term, millennial-length trends in resulting chronologies (Sect. 2.2). It is demonstrated that living trees and historical chronologies share a strong common signal though they are combined into a composite chronology. In Sect. 2.3, the climatic signal of the 1,244-year composite historical/living chronology is assessed by calibration with HISTALP instrumental temperature measurements. A discussion of the new record, and comparison with other alpine proxies and reconstructions are provided in Sect. 4.

2. Material, methods and results

2.1. The tree ring-data

The tree-ring widths (TRW) used in this study originate from the Briançonnais-Queyras-Embrunais region in the French Alps (44°45-45°00N, 6°30-6°45'E, **Fig. 1).** The sample material is derived from multi-centennial living trees (**Fig. 2A**) and also includes larch (*Larix decidua* Mill.) series from historical construction timbers (Edouard, 2007, 2008; Edouard and Thomas, 2008, **Fig**. **2B**). A total of 561 increment cores were collected, processed, and measured using standard dendrochronological techniques (Fritts, 1976). These cores include 185 samples from living or dead larch trees from 14 locations >2000 m, 336 samples from traditional buildings (mountain summer chalets and chapels) and 40 samples from an archaeological mining site (Freissinières-Grand Bois; **Py, 2009**). These historic larch timbers are located above 1900 m asl, excepted two chapels located at about 1600 m asl (Puy Saint Vincent).

From each living and dead tree, two to three cores were extracted with an increment borer at breast height on the cross-slope sides of the trunk. Sections were sampled on tumbledown or under restoration buildings in various parts of the wood structure: roof structure (beams, purlins, rafters), load-bearing walls, ceiling and floor joists. Individual series from a same tree (core and radius of a section) were first crossdated. Using both statistical and graphical programs, e.g. TSAP (Rinn, 1996) and Dendron II (Lambert, 2006, **Fig. 3**), the interannual ring-width variability within each mean-tree series was compared against all other series and against local or regional chronologies. Before the 14^{th} century, the millennium-long master chronology from the Merveilles valley (Mercantour, Serre 1979) was used as reference. This procedure is known as 'cross-dating' (a description of 'European style' cross-dating methodology is given in Schweingruber, 1988). In order to identify locally absent rings, eliminate measurement errors and ensure relative and absolute dating accuracy, the quality of the cross-dating was repeatedly checked with several statistical measurements (coefficient of correlation, coefficient of coincidence, Student's t test). Problematic samples, such as samples with missing rings or a distorted growth pattern, were dismissed from the data set. By including the dry dead and the samples from historical buildings, progressively older material could be cross-dated and, thus, the record of precisely dated tree rings could be extended back to 751AD while the outermost ring in the current sample of living trees was produced during the summer of 1995AD. However, the data are not continuous over the last 1250 years. A gap exists between 1304 and 1337AD.

First, series were combined on a site-by-site basis. Sample replication and chronology characteristics for each site and for both groups are detailed in **table 1.** The number of series per dataset varies considerably from 8 (Granon 3) to 323 (Névaches granges). The mean segment length (MSL) – the average number of rings per core or disc sample - ranges from 139 years (Puy-Saint-Vincent) to 458 (Echalp), with a mean of 270 years. These values are important since the segment lengths of the individual detrended series fundamentally limit the maximum wavelength of recoverable climatic information (Cook et al. 1995). Average growth rate of 0.82 mm/year varies between 0.61 mm/year (Oriol, Puy-Saint-André) and 2.57 mm (Pas d'Archail). Finally, the larch data were 'horizontally' split into two groups representing samples from living trees and historic construction wood, as these sub-samples considerably differ in: (i) the temporal distribution of the constituent series with older series,

before 1303AD sampled on historical buildings (**Fig 4A**); (ii) the average cambial age of the constituent tree rings for each year (**Fig. 4B**); (iii) their mean growth rates of 0.72 and 0.91 mm, (iv) and mean segment length of 290 and 178 years, respectively (**Tab. 1**). Hence, two standardization runs were calculated.

2.2. Standardization

The annual growth of a tree, manifest as tree-ring width (TRW), may in theory be attributed to a restricted number of different growth-controlling factors (Cook, 1990). In this study, sampled trees live close to their climatological limit of distribution and tree growth is assumed to be forced by two dominant factors: the climate (Tranquillini, 1979) and the age/size of individual trees. Non-climatic environmental factors will certainly have been important for individual trees at different times, but these factors are regarded as haphazard events with random distribution over space and time. To preserve long-timescale climate variability in long tree-ring chronologies while removing most of the age related variance, RCS was applied (e.g. Briffa et al. 1992). This is a so-called age-dependent composite detrending method, where (1) a given number of power transformed measurements are aligned by cambial age, (2) a single growth function [regional curve (RC), smoothed using a spline function of 10% the series length] is fit to the mean of all age-aligned measurements, and (3) the deviations of the measurements from this smoothed growth function are calculated as residuals (details in Esper et al. 2003). All detrended series are averaged to chronologies using the biweight robust mean (Cook and Kairiukstis, 1990). The variance is stabilized to minimize the effect of changing sample size using a technique that considers the number of samples per year and the cross-correlation between the single measurements (Osborn et al., 1997). The signal strength and confidence in the standardized chronologies is assessed by calculating R-BAR and expressed population signal (EPS) statistics in a 50-year window moved in 25- year steps over the total length of the series (Wigley et al., 1984). The R-BAR statistic is a measure of the average inter-correlation of all overlapping series, while EPS denotes the percent common signal. EPS is related to RBAR and to the number of replicate series, with EPS values above 0.85 generally regarded as satisfactory (Wigley et al., 1984).

While estimated TRW growth trends are remarkably similar for both groups (**Fig. 4 C, D**), a slight but systematic level offset between the TRW growth trends is seen. The RC based on the historic series indicates generally higher width compared to the RC of the living tree series, with largest differences found during juvenile growth. Resulting RCS chronologies of the historic and living trees measurements cover the 751–1894AD (with a gap between 1304 and 1337AD) and 1338–1995AD periods (**Fig. 5 A, B**). **Figure 5C, D** shows that the R-BAR values for the historic (mean: 0.48) and living tree chronology (mean: 0.45) are quite similar and the confidence in both chronologies is high, with EPS values typically above 0.85. In the historic chronology, EPS is on average 0.96, but with critically low values in some periods, particularly before 901 AD and 1210-1304 AD. In the living trees chronology, EPS is <0.85 between 1338 and 1413 AD.

Finally, after standardization, both RCS chronologies correlate at 0.57 over the well-replicated 1413–1894AD period of overlap and are merged for further analysis. The composite chronology, average of the two larch RCS chronologies, weighted by the number of series, is shown in **Fig. 5E**. After truncation at EPS>0.85, it covers the period 900-1210AD and 1413-1995AD.

2.3. Tree-growth response to climate

Monthly-homogenised records of temperature and precipitation from the HISTALP database (Auer et al. 2007) were used in order to identify climatic signals in the composite chronology and to investigate the optimum season for a climate reconstruction. This dataset consists in point values, gridded at 1°× 1° (temperature) and 0.1° x 0.1° (precipitation), lat × long, representing deviations from the 1961-90 mean. It results from a dense network of 134 meteorological stations, extends back to 1760 and covers the Greater Alpine Region (GAR, 4-19°E, 43-49°N, 0-3500m asl). We used its latest version, adjusted to take into account warm bias in summer temperature related to the insufficient sheltering of thermometers before 1850 (Böhm et al. submitted). Monthly mean series are calculated from 4 HISTALP points values (44-46°N, 6-7°E) enclosing the Briançonnais. Correlation coefficients between these 4 points over the 1760-2007 common period range from 0.89 to 0.99, demonstrating a rather homogenous climate field over the study area.

Correlation analyses using previous-year April to –year October monthly data and the RCS composite chronology were carried out. They give an indication of the direction and relative strength of the climatic forcing. The results show that TRW chronology has a significant positive response to June to August temperatures (**Fig. 6A).** JJA seasonal mean reveals highest correlations of 0.39. Moving 31-yr correlation analysis considering June, July, August and JJA indicates variable relationships for the individual monthly mean temperatures **(Fig. 6B).** Weaker correlations are obtained before 1880, and for August until 1940. Results for JJA are temporally more stable after 1880 and persistently significant at $p < 0.05$. No correlation with previous-year temperatures is significant at $p < 0.05$ and correlations with precipitation are weak.

A linear regression model was thus calibrated between JJA temperatures and the RCS composite chronology for the period 1760-1995. The fidelity of the reconstruction equation was tested in a calibration / verification exercise (Fritts, 1976; Cook and Kairiukstis, 1990) where the Histalp mean summer (JJA) temperature was split into two independent 117-year periods. A linear regression was fitted over the calibration period, and the derived coefficients applied to the tree ring data in the verification period **(Fig. 7A,B).** This scheme produces independent estimates of temperature that can be compared to the instrumental temperature data. The verification results were tested using the squared Pearson correlation (R^2), the reduction of error (RE) and the coefficient of efficiency (CE). The R^2 statistic, ranging from 0.0 to 1.0 is a measure of the proportion of variation explained by the regressor in the model. The RE and the CE statistics both range from minus infinity to +1.0 with RE > CE and where values greater than 0 give confidence to the model performance (Fritts, 1976; Briffa et al., 1988). Of these three statistics, CE is the most difficult to pass (Cook et al., 1994).

When the composite chronology is used in a linear regression, the R2, RE, CE, calibration and verification statistics against JJA mean temperatures indicate reconstructive skill against instrumental temperature data (**Tab. 2**), say r=0.42 and 0.48, RE=0.21, 0.27 and CE=0.20, 0.16. These calibration and verification statistics demonstrate some useful information preserved by the model (Cook et al., 1994). The mean discrepancy between reconstructed and instrumental temperatures is -0.3◦C (**Fig. 7A**) for the 1760-1995 period. Discrepancies are maximal at 1931 (+1.5◦C) and 1909 (-1.29◦C). When the curves are smoothed with a 10-year low-pass filter (**Fig. 7B**), r=0.62 and 0.71 for the calibration and verification periods, respectively. The maximal discrepancies occur around 1790, 1890 and 1970AD. Interestingly, no divergence with early instrumental data and during the last decades is found.

2.4. AD 751–1995 climate reconstruction

The reconstructions of summer temperature was made using regression weight for the Histalp June–August mean temperature and the full 1760–1995AD calibration period (**Tab. 2**). The reconstructions are expressed as temperature (1/10 °C) anomalies from the 1961-1990AD baseline period. The new reconstruction shows summer temperature variation in the Briançonnais region over the last 1,200 years with major confidence during the period's 900-1210AD and 1413-1995AD **(Fig 8A)**. The maximum amplitude is about 5°C with the warmest summers occurring around 1990AD and the coldest summers occurring around 1810AD. Figure 6A shows that, on the decadal-to-centennial timescales, notably cold periods occur around 850, 1150, 1520, 1590, 1650, 1690, 1810, 1910 and 1970AD. Notably warm periods occur around 1020, 1150, 1470 and 1990. The 60-year long warm period centred on 1150AD is especially noticeable while it appears as warm as the late twentieth century.

3. Discussion

3.1. Briançonnais climate history and possible bias in temperature reconstruction

A composite larch chronology is used to reconstruct past temperatures in the Briançonnais region until 751AD. This chronology yielded a high correlation to JJA summer temperatures (Tab. 2) as demonstrated by several authors (e.g. Serre, 1979; Carrer and Urbinati, 2004; Rolland et al., 1998; Frank and Esper, 2005).

The correlation significantly increases after smoothing the ring width record using a 10-year low pass filter. This shift is related to the periodic (8–9 years) population waves of the larch budmoth (LBM, *Zeiraphera diniana* Guénée) and their feeding on needles, which typically cause growth reductions in

the year and generally subsequent years from the attack and affect the climatic signal particularly in the higher frequency, inter-annual domain. For this reason, the climate description was only conducted in the medium frequency domain.

The Briançonnais temperature history reports warm summers during much of the tenth, twelfth and late thirteenth centuries (Fig. 6E) commonly associated with the late Medieval Warm Period (Hughes and Diaz, 1994; Esper et al. 2002). This period, associated with the Medieval Warm Period, is characterized by significant inter-decadal temperature variations, with warm decades centered around 1020, 1160 and 1240. High summer temperatures are also inferred prior to AD 1000, but caution with this observation is warranted as this period is characterized by low sample replication **(Fig.8A)** and low EPS values.

In our reconstruction, the Little Ice Age (LIA) is well marked and the cold period extends from 1500 to 1850AD but the transition MWP-LIA remains temporally imprecise due to the gap and the associated uncertainties in the reconstruction between 1220 and 1420AD. Cooler conditions during the LIA are accompanied by significant inter-decadal variations. Low temperatures are reconstructed in the 1520s, around 1600, around 1700 and 1815–1820. The inter-decadal variations seen since 1760AD are in line with JJA temperatures recorded in the Alps (Fig. 7A,B). We do not notice any misfit between colder reconstruction and warmer instrumental data before ~1840AD as related in several papers (Büntgen et al., 2005, 2006; Frank et al., 2007; Corona et al., 2008, 2010). This improvement may be related to the adjustments made on the HISTALP dataset to take into account sheltering-related biases before 1850AD.

Since the 1820s, temperatures increased until the end of the record in 1995AD. Because of uncertainties in the proxy-instrumental temperature calibration, it is still difficult to unequivocally assert that the late 20th century warming is significantly greater than the peak warmth of the Medieval Warm Period. But there is even less justification to assert the opposite–it is not possible to make a robust statement that the Medieval Warm Period was warmer than the last two decades of the 20th century.

3.2. Comparison with other climate reconstructions

Among the previous reconstructions of late-Holocene climate changes available in the Alps, we selected, as reference climate records to validate the Briançonnais temperature reconstruction: (i) the Great Aletsch glacier history (Holzhauser et al., 2005); (ii) the Lake Anterne temperature reconstruction derived from chironomid assemblages (Millet et al., 2009); (iii) the speleothem-based temperature reconstruction in Spannagel Cave (Austria, Mangini et al., 2005); (iv) the reconstruction of River Rhône flooding activity from Lake Bourget (Arnaud et al., 2005); (v) the summer temperatures reconstructed from larch TRW and Maximum Density (MXD) series from the Swiss and Austrian Alps (Büntgen et al., 2005, 2006),

Past variations in the length of the Great Aletsch glacier are well-documented over the last 3500 years on the basis of tree-ring studies of subfossil wood found in situ in the glacier forefield and its surroundings. This chronology is supported by radiocarbon and tree-ring dating, moraine studies and annual direct observations since 1892 (Holzhauser et al., 2005). In Lake Anterne (2060 m asl), Millet et al. (2009) presented a chironomid-based reconstruction of late-Holocene temperature. Chironomid assemblages were studied in 49 samples along an 8 m long sediment core covering the last 1800 years. July air temperatures were inferred using an inference model based on the distribution of chironomid assemblages in 100 Swiss lakes. The Mangini summer reconstruction is based on the precisely dated isotopic composition of a stalagmite from Spannagel Cave (2524 m asl) in the Central Alps of Austria. The stalagmite was dated using the U/Th method and δ18O profile was converted into yearly temperatures. Despite it concerns the whole year, this reconstruction is used for comparison because it is fully independent from our dataset. In Lake Bourget, Arnaud et al. (2005) reconstructed the Holocene evolution of the River Rhône flooding activity by measuring the typical mineralogical fraction transported by the river and diluted by the autochthonous carbonate fraction within the lake. This series covers the last 7200 years and was dated with nine AMS 14C measurements. Finally, annually resolved summer temperatures were reconstructed for the European Alps at high temporal resolution by Buntgen et al. (2005, 2006). The reconstructions repectively cover the periods 951-2003AD (755–2004AD) and are based on recent and historical larch ring width (maximum density) series.

Changes in tree-ring-inferred temperatures were within the prediction error of the model. However, the decadal to centennial temperature variability inferred from the Briançonnais tree-ring composite chronology matches the climate history inferred from other proxies in the northern and central Alps (Fig. 8) as follows:

• The high temperatures reconstructed in the Briançonnais between 900 and 1200AD match with a major glacier retreat in the northern Alps, a period of reduced Rhône flooding activity and high temperature reconstructed from chironomids, speleothems and larch series. In the detail, between 1020 and 1180AD, the tree-ring reconstructions are remarkably synchronous with a cold phase in the mid-11th century and hot summers reconstructed around 1180AD. The sharp decline in the reconstructed temperatures around 1050AD is related to the Oort solar minimum (Büntgen et al. 2006). It is in phase with the beginning of a Great Aletsch glacier advance event reported by Holzhauser et al. (2005) but is observed neither in speleothems nor in lake sediments. Between 1150 and 1220AD, hot summers reconstructed from tree-rings coincide with a peak in July temperatures reconstructed from chironomid assemblages in lake Anterne (Millet et al. 2009) and predate a major phase of glacier advance (1250AD).

• The LIA lasting from 1500 to 1850AD in the Briançonnais coincides with an Alpine glacier re-advance, a period of increased sediment supply in Lake Bourget and a decrease in summer temperature reconstructed from other speleothems, chironomid assemblages and alpine larch series (Fig. 8). The cold period that occurs around 1690AD is also visible in other proxies and particularly with a major period of glacial advance and flooding activity. This so-called Maunder minimum period coincides with an enhanced concentration in atmospheric 14C (Stuiver and Braziunas, 1993), several large volcanic eruptions (Briffa et al., 1998), a reduced solar activity, and a low number of sunspots (Spörer, 1887; Maunder, 1922; Eddy, 1976; Lean et al., 1995). During the Dalton solar minimlum (1810), a series of tropical eruptions (1808–15), likely resulted in an aerosol-accumulated summer cooling effect (Chenoweth 2001; Dai et al.1991). This volcanic forcing has been demonstrated to be largely responsible for the drop recorded in tree-ring series and glacier advance whereas changes in solar forcing and the increasing atmospheric CO2 concentrations were of minor importance (Wagner and Zorita, 2005).

• Since the mid-18th century, the Briançonnais temperature reconstruction tracks the post LIA warming recorded in meteorological series (Fig. 7) and attributed to the increasing forcing induced by human activities (Wanner et al. 2008), such as rapid land cover change, increase of greenhouse gases and aerosols, and stratospheric ozone depletion. This evolution is synchronous with the Great Aletsch Glacier retreat and is recorded in many other climatic records from the Alpine region (e.g., Holzhauser et al., 2005; Mangini et al., 2005).

Conclusion

In the Briançonnais, the tree-ring reconstruction of summer temperature indicates a high variability of summer temperature in the northern French Alps during the last 1250 years. At a hemispheric or global scale the existence of the LIA and MWP have been questioned (Jones and Mann, 2004). The present temperature reconstruction, however, together with the reconstruction of Alpine glacier fluctuations, major Rhône river flooding activity, summer temperature derived from *Larix decidua*, speleothems and chironomid assemblages confirm the existence of several significant climatic changes during the last 1250 years in the French Alps and more specifically the MWP and the LIA.

Moreover, the Briançonnais reconstruction indicates a relatively high magnitude of change in the inferred summer temperature. The temperatures reconstructed during the hottest periods of the MWP reach values close to the 1980–1995 mean JJA temperature. In comparison with conditions prevailing during MWP, the LIA coldest events were characterized by a cooling of about 1.5 (Maunder Minimum) and 1.3°C (Dalton Minimum). These results match well with the magnitude of temperature changes reconstructed in the Alps for the LIA cooling from other proxies, such as oxygen isotopic composition in speleothems (Mangini et al., 2005) and the *Larix decidua* ring width and density series (Büntgen et al., 2005, 2006).

A detailed discussion of the relationship between human society and climate, the complexity of which has been stressed by previous studies (e.g., Berglund, 2003), lies well beyond the scope of this article. However, the results obtained in the Briançonnais provide the opportunity to briefly point to the possibility of impacts of climate variations on human activities in such an elevated Alpine area. Several authors have already discussed the coincidence of climatic reversals and reduced human activity in

sensitive regions (e.g. Berglund, 2003). In the Briançonnais, large fluctuations in summer temperature as shown in this study might have at least partly influenced the land-use activities in alpine high-elevation sites. Thus, the lack of archeological wood around 1300AD coincides with the transition between MWP and LIA recorded in other proxies, says a major advance in Grindewald glacier length and a strong cooling recorded in chironomid assemblages from Lake Anterne, tree-ring series in Central Europe and oxygen isotopic composition in speleothems. Interestingly, this period also corresponds to the end of mining activities in the high altitude mine of Brandes (neighbouring Oisans massif) probably triggered by increasing environmental and climatic constraints (Bailly-Maître, 1996).

Captions

Figure 1. Localisation map of the tree-ring sites used for the reconstruction. All tree-ring sites are above 1900 m asl excepted Puy-Saint-Vincent.

Figure 2. Multi-centennial living larches in the upper part of the Oriol forest (A) and bearing wall of a mountain summer barn composed of a typical assemblage of larch boles, wood pieces on wood pieces (Névache, Hautes-Alpes).

Table 1. Characteristics of the tree-ring sites: site name, location, period covered by the chronology, exposition, number of individual tree-ring width series (Nb series), Mean Serie Length (MSL in years), Average Growth Rate (AGR in mm) and source (DENDRODB: http:// dendrodb.cerege.fr).

Figure 3. Correlation matrix of the tree ring series from the Buffères buildings and local or regional master chronologies (Dendron II software).

Figure 4. A. Temporal distribution of the 376 historical (blue) and 185 living trees (red) samples ordered by calendar age of their innermost ring. B. Mean cambial age of the historical and living trees samples for each calendar year. C, D. Regional curves (RCs) of the age-aligned living trees (C) and historical (D) TRW series. The number of replicate series for each year (the sample depth) is shaded in grey.

Figure 5. Fig. 5 RCS standardized chronologies for historic (blue, A), living trees (red, B) and composite TRW (black, E), with their corresponding EPS (C) and r-bar (D) values plotted for 50-year windows with 25 years overlap. The number of replicate series for each year (the sample depth) is shaded in grey.

Figure 6. Climate response of the composite RCS chronology. (A) Correlations with the HISTALP monthly mean temperatures (black) and precipitation (gray) of the previous and current year (1760-1995). [(B), inset to a] Moving 31-year correlations with current-year June (light grey), July (dark grey), August (black), and JJA (dotted black) mean temperatures. Horizontal lines denote 95% and 99% significance levels.

Table 2. Calibration and verification results

Figure 7. The regression equation was tested in a cross calibration/verification exercise using the RCS-chronology and the HISTALP mean summer (June–August) temperature. The data were split in two 118-year periods: 1760–1877 and 1878–1878. The regression coefficients derived from the first period were used to reconstruct temperatures in the second period, and vice versa, thus producing two sets of independent data. The instrumental temperature is shown in blue and estimates in red for unfiltered and 20-year low pass dataset.

Figure 8. Comparison of the Briançonnais reconstruction with regional temperature reconstructions. All reconstructions were 20-yr low-pass filtered. (A) our raw (grey) and low-pass filtered (black) reconstruction is compared with : (B) the advance/retreat history of the Great Aletsch glacier (Switzerland, Holzhauser et al., 2005); (C) the chironomid-based temperature reconstruction at Lake Anterne (France, Millet et al., 2009) and the speleothem-based temperature reconstruction in Spannagel Cave (Austria, Mangini et al., 2005); (D) the reconstruction of River Rhône flooding activity from Lake Bourget (France, Arnaud et al., 2005); (E) the Alpine temperatures derived from *Larix decidua* ring width and wood density series (Büntgen et al., 2006). All tree-ring temperature reconstructions were transformed to z scores over the 951–1995AD common period.

References

Arnaud F., Revel-Rolland M., Chapron E., Desmet M., Tribovillard, N. 2005. 7200 years of Rhône river flooding activity recorded in Lake Le Bourget: a high resolution sediment record of NW Alps hydrology. The Holocene, 15, pp. 420-428.

Bailly-Maitre M.C., 1996. Brandes-en-Oisans: incidences d'un milieu montagnard sur une exploitation minière médiévale, colloque de la Société d'Archéologie Médiévale. In Colardelle, M., editor,L'homme et la nature au Moyen Age (paléoenvironnement et sociétés européennes). Errance, pp. 235-245.

Berglund, B.E. 2003: Human impact and climate changes – synchronous events and a causal link? Quaternary International,105, pp. 7-12.

Böhm R., Jones P.D., Hiebl J., Frank D., Brunetti M., and Maugeri M. submitted. The early instrumental warm-bais: a solution for long central European temperature series 1760-2007. Climatic change.

Briffa K.R., Jones P.D., Pilcher J.R., Hughes M.K., 1988. Reconstructing summer temperatures in northern Fennoscandia back to A.D. 1700 using tree-ring data from Scots pine. Arctic and Alpine Research, 20, pp. 385-394

Briffa K.R., 1992. Increasing productivity of ''natural growth'' conifers in Europe over the last century. In: Bartholin T.S., Berglund B.E., Eckstein, D., Scheiwngruber F.H. (eds) Tree rings and environment. Ystad, Sweden, pp 64–71.

Briffa K.R., Jones P.D., Bartholin T.S., Osborn T.J., 1998. Influence of volcanic eruptions on Northern Hemisphere summer temperature over the past 600 years. Nature, 393, pp. 450-455.

Büntgen U., Frank D.C., Nievergelt D., Esper J., 2006. Summer temperature variations in the European Alps, AD 755-2004. Journal of Climate 19, pp.5606–5623.

Büntgen U., Frank D.C., Grudd H., Esper J., 2008. Long-term summer temperature variations in the Pyrenees. Climate dynamics, DOI 10.1007/s00382-008-0390-x.

Carrer M., Urbinati C., 2004. Age-dependent tree-ring growth responses to climate in *Larix decidua* and *Pinus cembra*. Ecology 85, p. 730–740.

Chenoweth M., 2001. Two major volcanic cooling periods derived from global marine air temperature, AD 1807-1827. Geophysical Research Letters, 28, pp. 2963-2966.

Cook E.R.,1990. A conceptual linear aggregate model for tree rings. In: Cook E, Kairiukstis L (eds) Methods of dendrochronology: applications in the environmental science. Kluver Academic Publishers, Dordrecht, 394p.

Cook E.R., Kairiukstis L.A., 1990. Methods of dendrochronology: applications in the environmental science. Kluwer Academic Publishers, Dordrecht, 394p.

Cook E.R., Briffa K.R., Meko D.M., Graybill D.A., Funkhouser G., 1995. The 'segment length curse' in long tree-ring chronology development for palaeoclimatic studies. The Holocene, 5, pp. 229–237.

Cook E.R., Briffa K.R., Jones P.D., 1994. Spatial regression methods in dendroclimatology: a review and comparison of two techniques. International Journal of Climatology, 14, pp. 379-402.

Corona C., Guiot J., Edouard J.-L., Chalié F., Büntgen U., Nola P., Urbinati C., 2008. Millennium-long summer temperature variations in the European Alps as reconstructed from tree rings, Climate of the past discussion, 4, pp. 1159-1201.

Corona C, Edouard J.L., Guibal F., Guiot J., Bernard S., Thomas A., Denelle N., 2010. Long-term summer (751-2008) temperature fluctuation in the French Alps based on tree-ring data. Boreas, accepted.

Dai J., Mosley-Thompson E., Thompson L.G., 1991. Ice core evidence for an explosive tropical volcanic eruption 6 years preceding Tambora. Journal of Geophysical Research, 96, pp. 361–17 366.

Eddy J.A., 1976. The Maunder Minimum, Science, 192, pp. 1189-1202.

Edouard J.-L., 2007. Les très vieux arbres vivants et les arbres morts, témoins et vestiges des forêts du passé dans les Alpes du Sud : lecture dendrochronologique d'un patrimoine naturelle et humain. In Bernardi P. (ed.) Forêts alpines et charpentes méditerranéennes, édition du Fournel, L'Argentière La Bessée, pp. 9-16.

Edouard J.-L., 2008. Données nouvelles sur l'histoire de la Chapelle Saint Hippolyte (Névache, Hautes-Alpes, France). Apport de la datation dendrochronologique. Revue de la Société d'Etude des Hautes-Alpes, p. 37-52.

Edouard J.-L., Thomas A., 2008. Cernes d'arbres et chronologie holocène dans les Alpes françaises. In Actes du colloque GDR JURALP, Desmet M., Magny M., Mocci F. (eds.) « Du climat à l'Homme. Dynamique holocène de l'environnement dans le Jura et les Alpes », Aix-en-Provence, 15-16 novembre 2007. Cahiers de Géographie, collection Edytem 6, pp. 179-190.

Esper J., Cook E.R., Schweingruber F.H., 2002. Low-frequency signals in long tree-ring chronologies for reconstructing past temperature variability, Science, 295 pp. 2250-2253.

Frank D., Esper J., 2005. Temperature reconstructions and comparisons with instrumental data from a tree-ring network for the European Alps. International Journal of Climatology, 25, pp. 1437–1454.

Frank D., Büntgen U., Böhm R., Maugeri M., Esper J., 2007. Warmer early instrumental measurements versus colder reconstructed temperatures: shooting at a moving target. Quaternary Science Review, 28, pp. 3298–3310.

Fritts H.C., 1976. Tree rings and climate, London, 567 p.

Grove, J.M., 1988. The little ice age, Methuen, New-York, 498p.

Holzhauser H., Magny M., Zumbühl H.J., 2005. Glacier and lake-level variations in west-central Europe over the last 3500 years. The Holocene 15, p. 789–801.

Hughes M.K., Diaz H.F., 1994. Was there a ''Medieval Warm Period'', and if so, where and when? Climate Change, 26, pp. 109-142.

Jansen E., Overpeck J., Briffa K.R., Duplessy J.C., Joos F., Masson-Delmotte V., Olago D., Otto Bliesner B., Peltier W.R., Rahmstorf S., Ramesh D., Raynaud D., Rind D., Solomina O., Villalba R., Zhang D., 2007.

Palaeoclimate, in Solomon S., Qin D., Manning M., Chen Z., Marquis M., Averyt K.B., Tignor M., Miller H.L. (Eds.), Climate Change 2007: The Physical Science Basis. Contribution of Working Group I to the Fourth Assesement Report of the Intergovernmental Panel on Climate Change. Cambridge University Press, Cambridge and New York,
Jones P.D., Mann M.E., 2004. Climate over past millennia. Reviews of Geophysics 42, pp. 1-42.
Lamb H.H.,1977. Climate, Present, Past and Future: Volume 2. Climatic History and the future. Methuen: London, 835 p.
Lambert G.-N., 2006. Dendrochronologie, Histoire et Archéologie, modélisation du temps. Le logiciel Dendron II et le projet Historic Oaks. Habilitation à Diriger des Recherches, University of Franche-Comté, Besançon, 2 vol., 152 p et 206 p.
Lean J., Beer J., Bradley R. S., 1995. Reconstruction of Solar Irradiance since 1610: Implications for Climate Change, Geophysical Research Letters, 22, pp. 3195–3198.
Mangini A., Spötl C., Verdes P., 2005. Reconstruction of temperature in the Central Alps during the past 2000 yr from a d18O stalagmite record. Earth and Planetary Science Letters, 235, pp. 741–751.
Maunder E. W., 1922. 'The Prolonged Sunspot Minimum 1675–1715', British Astronomy Association Journal, 32, pp. 140–145
Millet L., Arnaud F., Heiry O., Magny M., Verneaux V., Desmet M., 2009. Late-Holocene summer temperature reconstruction from chironomid assemblages of Lake Anterne,The Holocene, 19, pp. 317-328.
Nicolussi K., Schiessling P., 2001. Establishing a multi-millenial Pinus cembra chronology for the central Eastern Alps. In International Conference of Tree-Rings and People, Kaennel Dobbertin M, Bräker O.U. (eds), Davos, 22 – 26 September 2001. Abstracts. Swiss Federal Research Institute WSL, Birmensdorf, pp. 87.
Osborn T.J., Briffa K.R., and Jones P.D., 1997. Adjusting variance for sample size in tree-ring chronologies and other regional-mean time series. Dendrochronologia, 15, pp. 89–99.
Py V., 2009. (à compléter)
Rinn F., 1996. TSAP Reference Manual, Version 3.0, Heidelberg, 263 p.
Rolland C., Petitcolas V., Michalet R., 1998. Changes in radial tree growth for *Picea abies, Larix decidua, Pinus cembra* and *Pinus uncinata* near the alpine timberline since 1750. Trees,13, pp. 40–53
Schweingrüber F.-H., 1988. Tree-rings - Basics and applications of dendrochronology, Dordrecht, 277 p.
Serre F., 1979. The dendroclimatological value of European larch (*Larix Decidua* Mill.) in the French Maritime Alps. Tree-Ring Bulletin, 38, pp. 25-34.
Spörer F.W.G., 1887. 'Über die Periodizität der Sonnenflecken seit dem Jahre 1618, vornehmlich in Bezug auf die heliographische Breite derselben, und Hinweis auf eine erhebliche Störung dieser Periodizität während eines langen Zeitraumes', Vjschr. Astron. Ges. Leipzig, 22, pp. 323–329.
Stuiver M., Braziunas T.F., 1993. Sun, ocean, climate and atmospheric 14CO2: an evaluation of causal and spectral relationships. The Holocene, 3, pp. 289–305.
Tranquillini W., 1979. Physiological ecology of the alpine timberline. Springer, Berlin, 131p.
Wagner S., Zorita E., 2005. The influence of volcanic, solar and CO2 forcing on the temperatures in the Dalton Minimum (1790–1830) : A model study. Climate Dynamics, 25, pp. 205-218.
Wanner H., Beer J., Bütikofer J., Crowley T.J., Cubasch U., Flückiger J., Goosse H., Grosjean M., Joos F., Kaplan J.O., Küttel M., Müller S.A., Prentice C., Solomina O., Stocker T.F., Tarasov P., Wagner M., Widmann M., 2008. Mid- to Late Holocene climate change: an overview. Quaternary Science Reviews 27, pp. 1791–1828.
Wigley T. M. L., Briffa K.R., and Jones P.D., 1984. On the average of value of correlated time series, with applications in dendroclimatology and hydrometeorology. Journal of Climate and Applied Meteorology, 23, pp. 201–213.

Site	Species	Longitude (E)	Latitude (N)	Altitude (m a.s.l)	Period (AD)	Nb series	MSL (years)	AGR (mm/year)	Source
Bois des Bans	LADE	6,7038	44,9168	2000	1640-1995	13	269	0.7	Guibal. DENDRODB
Chardonnet	LADE	6,53861	45,0294	2180	1491-1989	18	372	0.67	Edouard
Clapouse	LADE	6,43057	44,8678	2150	1557-1995	16	289	0.77	Guibal. DENDRODB
Echalp	LADE	7,00056	44,7612	1930	1338-1995	24	458	0.8	Edouard
Fressinières-Grand Bois 1	LADE	6,5047	44,7255	1990	1542-1990	21	317	0.75	Edouard
Fressinières-Grand Bois 2	LADE	6,5047	44,7256	1930	778-1214 1474-1992	40	236	1.35	Edouard
Granon 1	LADE	6,63197	44,9731	2230	1710-1993	12	228	0.88	Petitcolas. DENDRODB
Granon 3	LADE	6,61771	44,9692	2250	1734-1993	8	222	0.65	Petitcolas. DENDRODB
Izoard	LADE	6,73177	44,8386	2150	1734-1993	12	229	0.69	Petitcolas. DENDRODB
Le Melezein	LADE	6,63184	44,8652	2150	1752-1995	13	188	1.17	Guibal. DENDRODB
Les Clots	LADE	6,46683	44,816	2100	1749-1995	15	192	1.35	Guibal. DENDRODB
Nevache granges	LADE	6,548	45,0258	2030	751-1303 1357-1894	323	159	0.74	Edouard
Oriol	LADE	6,59861	44,7961	2180	1381-1989	19	446	0.61	Edouard
Puy Saint André	LADE	6,56666	44,88333	2300	1651-1994	14	274	0.61	Guibal. DENDRODB
Puy Saint Vincent	LADE	6,48611	44,83027	1600	923-1186	13	139	0.7	Edouard
Historical series	LADE	6.48-6.55	44.79-44.98	1600-2030	751-1303 1357-1894	376	178	0.72	
Living trees series	LADE	6.43-7.00	44.72-45.02	1930-2300	1381-1995	185	290	0.93	
Composite series	LADE	6.43-7.00	44.72-45.02	1600-2300	751-1303 1357-1995	561	178	0.83	

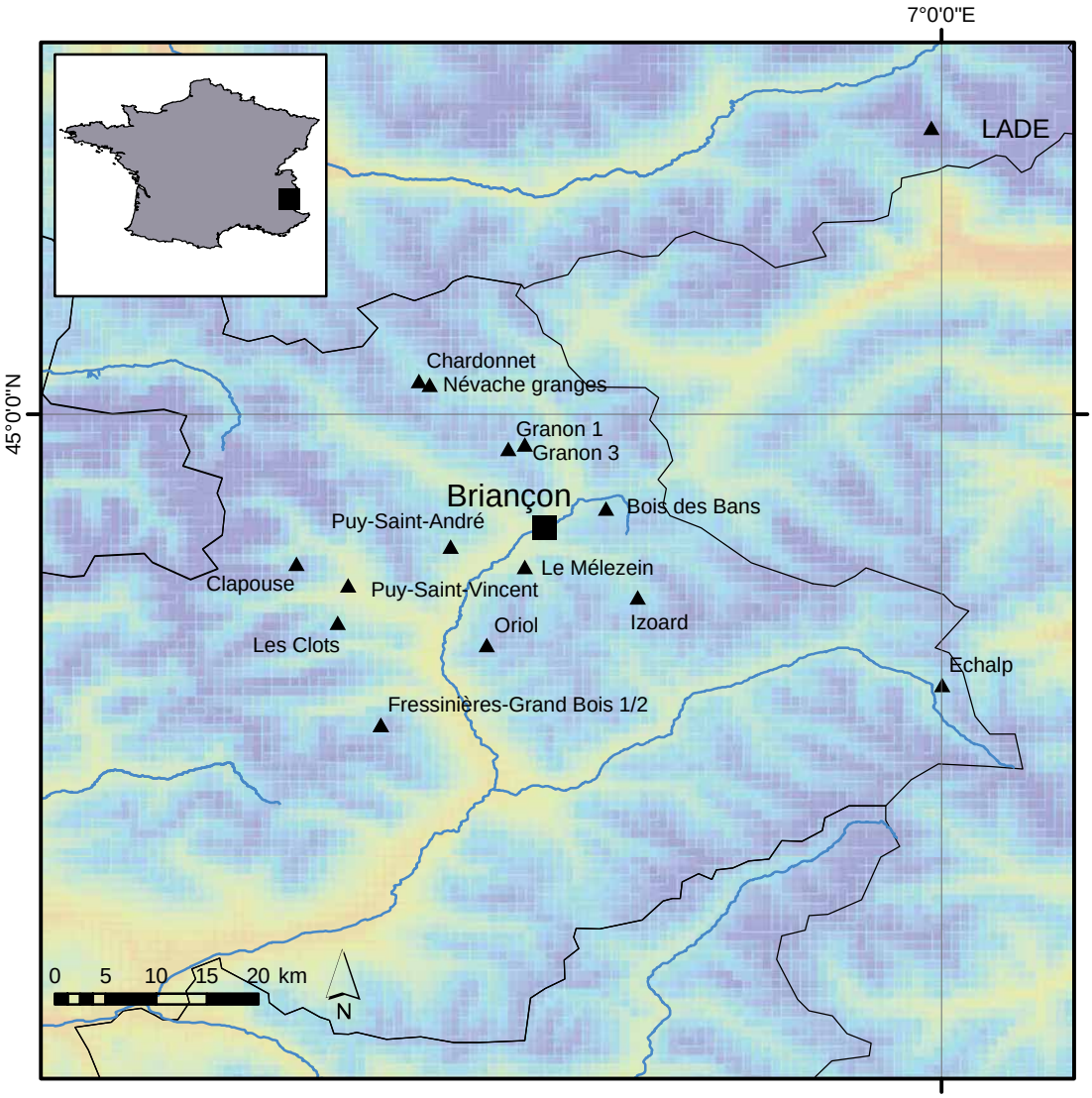
7°0'0"E
45°0'0"N
LADE
Chardonnet
Névache granges
Granon 1
Granon 3
Briançon
Bois des Bans
Puy-Saint-André
Le Mélezein
Clapouse
Puy-Saint-Vincent
Izoard
Oriol
Les Clots
Echalp
Fressinières-Grand Bois 1/2
0 5 10 15 20 km
N


A


B

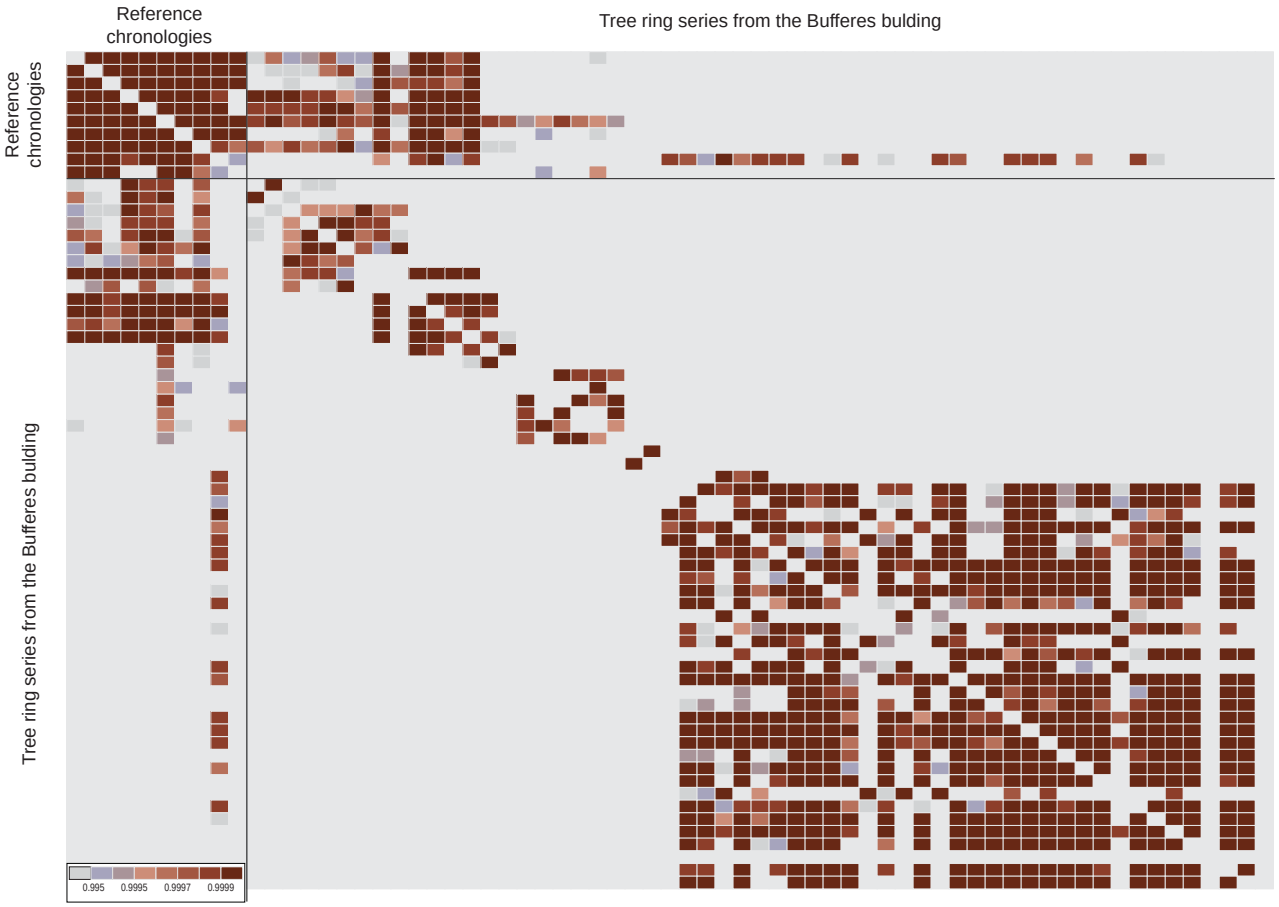
Reference chronologies
Tree ring series from the Bufferes bulding
Reference chronologies
Tree ring series from the Bufferes bulding
0.995
0.9995
0.9997
0.9999

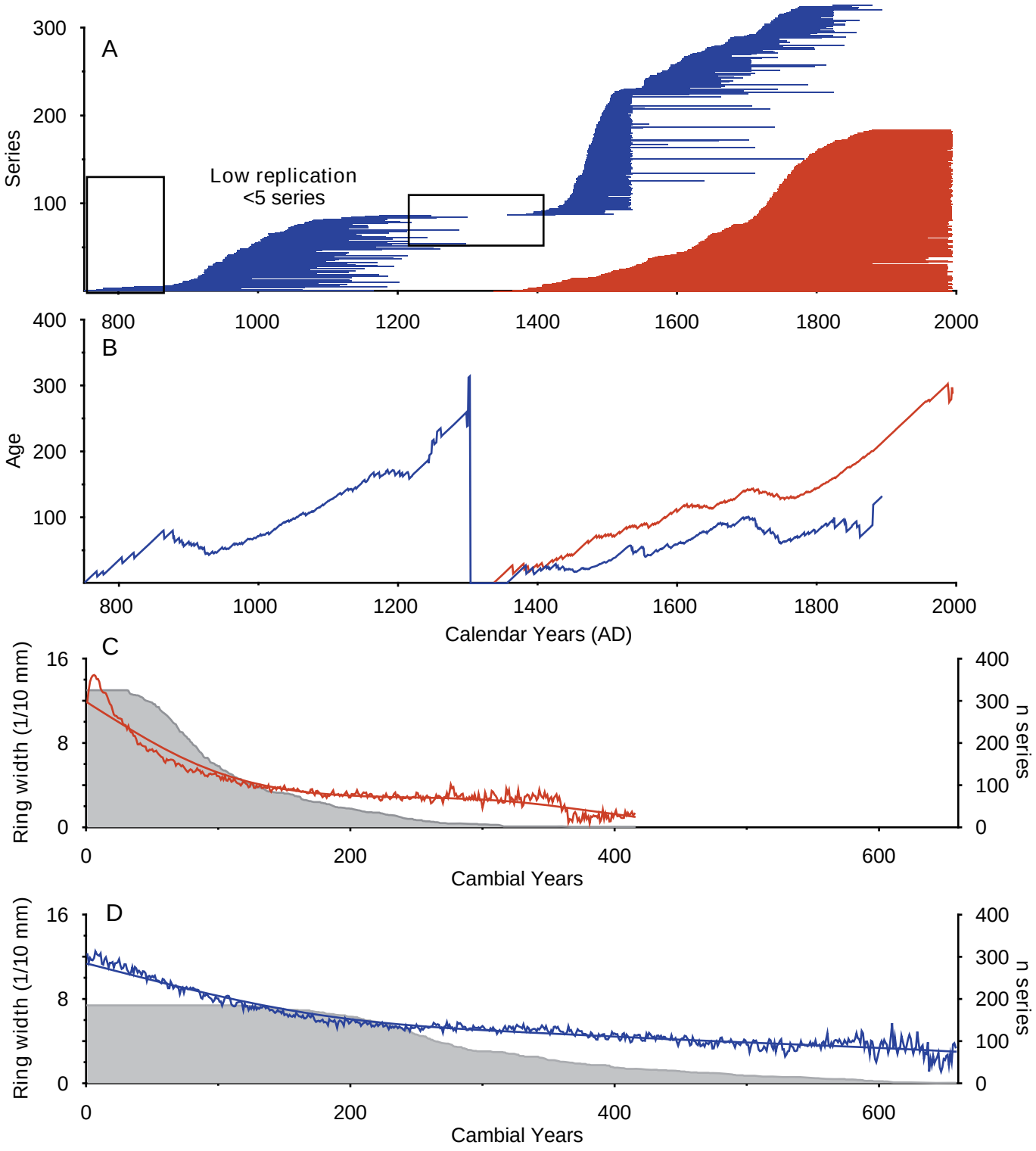
A
Series
300
200
100
Low replication
<5 series
400
800
1000
1200
1400
1600
1800
2000
B
Age
300
200
100
800
1000
1200
1400
1600
1800
2000
Calendar Years (AD)
C
Ring width (1/10 mm)
16
8
0
400
300
200
100
0
n series
0
200
400
600
Cambial Years
D
Ring width (1/10 mm)
16
8
0
400
300
200
100
0
n series
0
200
400
600
Cambial Years

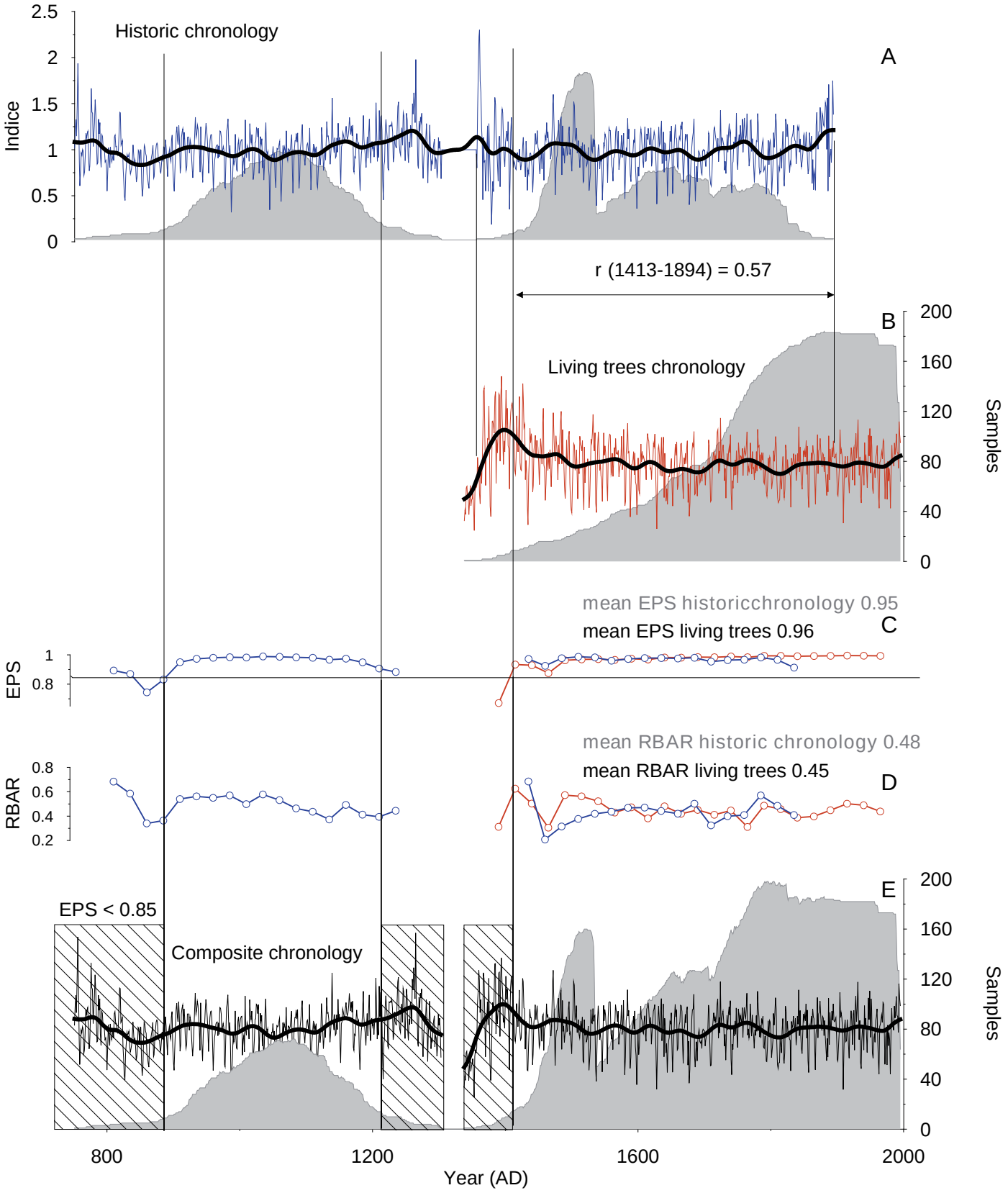
Historic chronology
A
Indice
2.5
2
1.5
1
0.5
0
r (1413-1894) = 0.57
B
Living trees chronology
200
160
120
80
40
0
Samples
mean EPS historicchronology 0.95
mean EPS living trees 0.96
C
EPS
1
0.8
mean RBAR historic chronology 0.48
mean RBAR living trees 0.45
D
RBAR
0.8
0.6
0.4
0.2
EPS < 0.85
Composite chronology
E
200
160
120
80
40
0
Samples
800
1200
1600
2000
Year (AD)

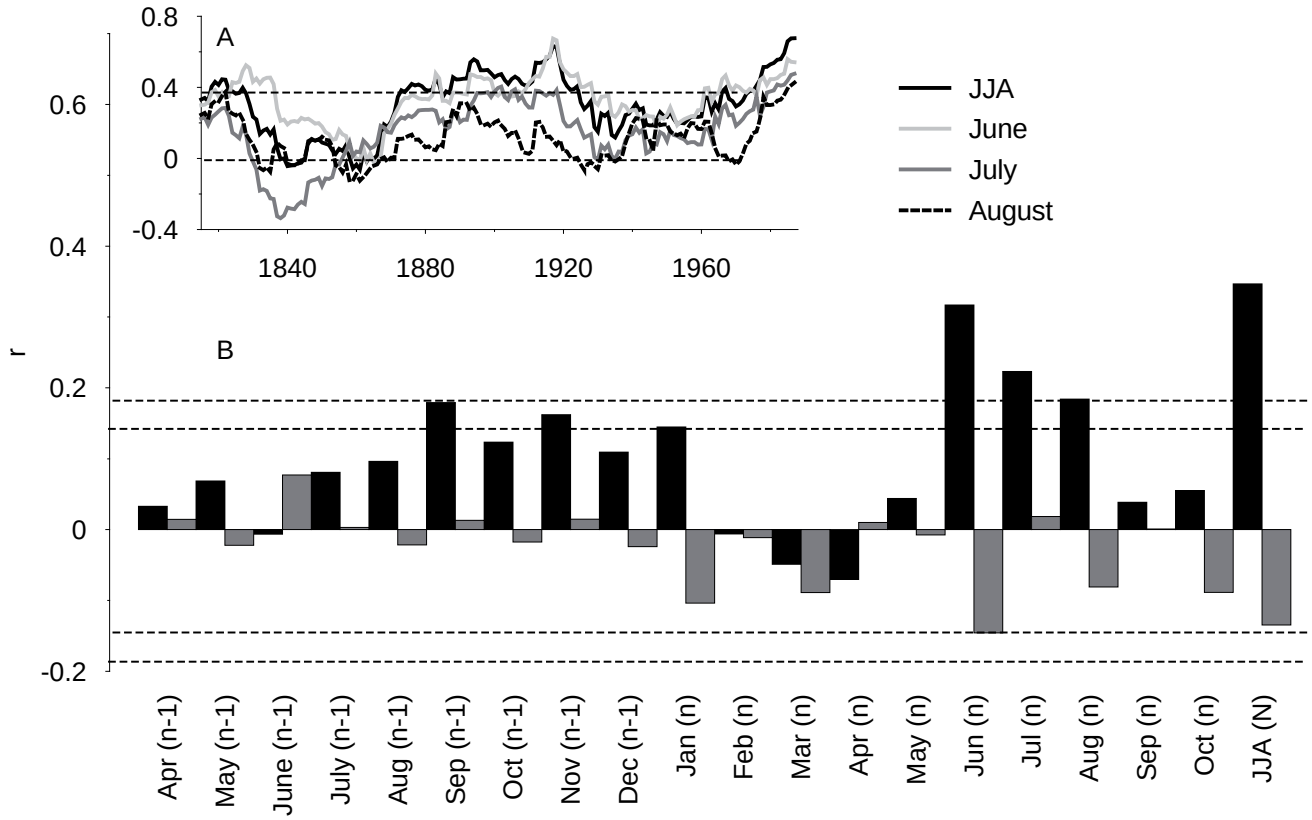
A
B
r
0.8
0.4
0
-0.4
0.6
0.4
0.2
0
-0.2
1840
1880
1920
1960
JJA
June
July
August
Apr (n-1)
May (n-1)
June (n-1)
July (n-1)
Aug (n-1)
Sep (n-1)
Oct (n-1)
Nov (n-1)
Dec (n-1)
Jan (n)
Feb (n)
Mar (n)
Apr (n)
May (n)
Jun (n)
Jul (n)
Aug (n)
Sep (n)
Oct (n)
JJA (N)

Calibration period	1760-1877	1878-1995	1760-1995
Correlation *R*	0.42	0.48	0.45
Explained Variance R^2	0.18	0.24	0.21
Observations	118	118	236
Regression weights			
TRW_t	21.54	22.03	21.96
Constant	-25.16	-24.23	-24.88
Verification period	1878-1995	1760-1877	
Explained Variance R^2	0.24	0.18	
Reduction of Error RE	0.24	0.27	
Coeff. of efficiency CE	0.20	0.16	

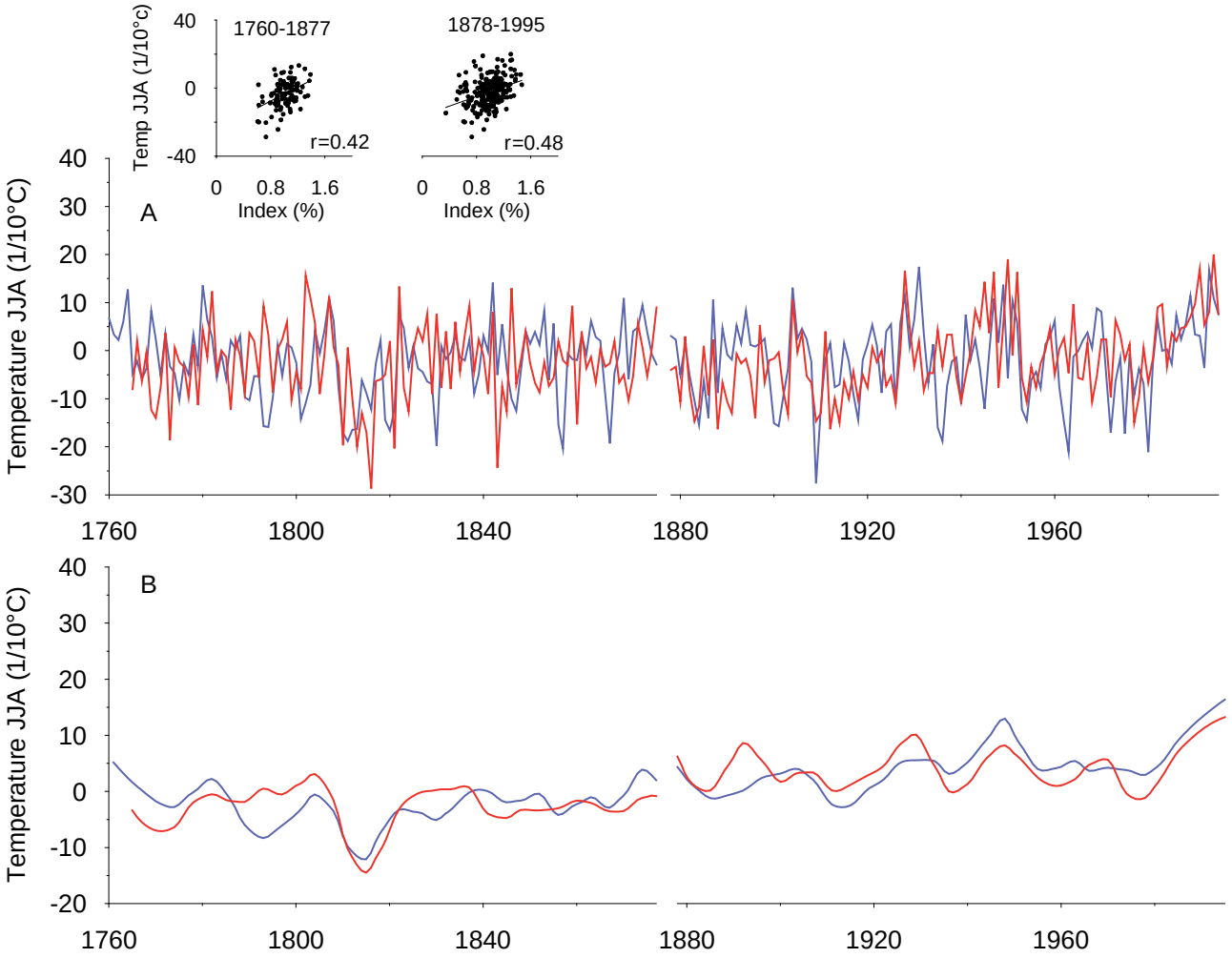
Temp JJA (1/10°c)
40
0
-40
1760-1877
r=0.42
0
0.8
1.6
Index (%)
1878-1995
r=0.48
0
0.8
1.6
Index (%)
A
Temperature JJA (1/10°C)
40
30
20
10
0
-10
-20
-30
1760
1800
1840
1880
1920
1960
B
Temperature JJA (1/10°C)
40
30
20
10
0
-10
-20
1760
1800
1840
1880
1920
1960

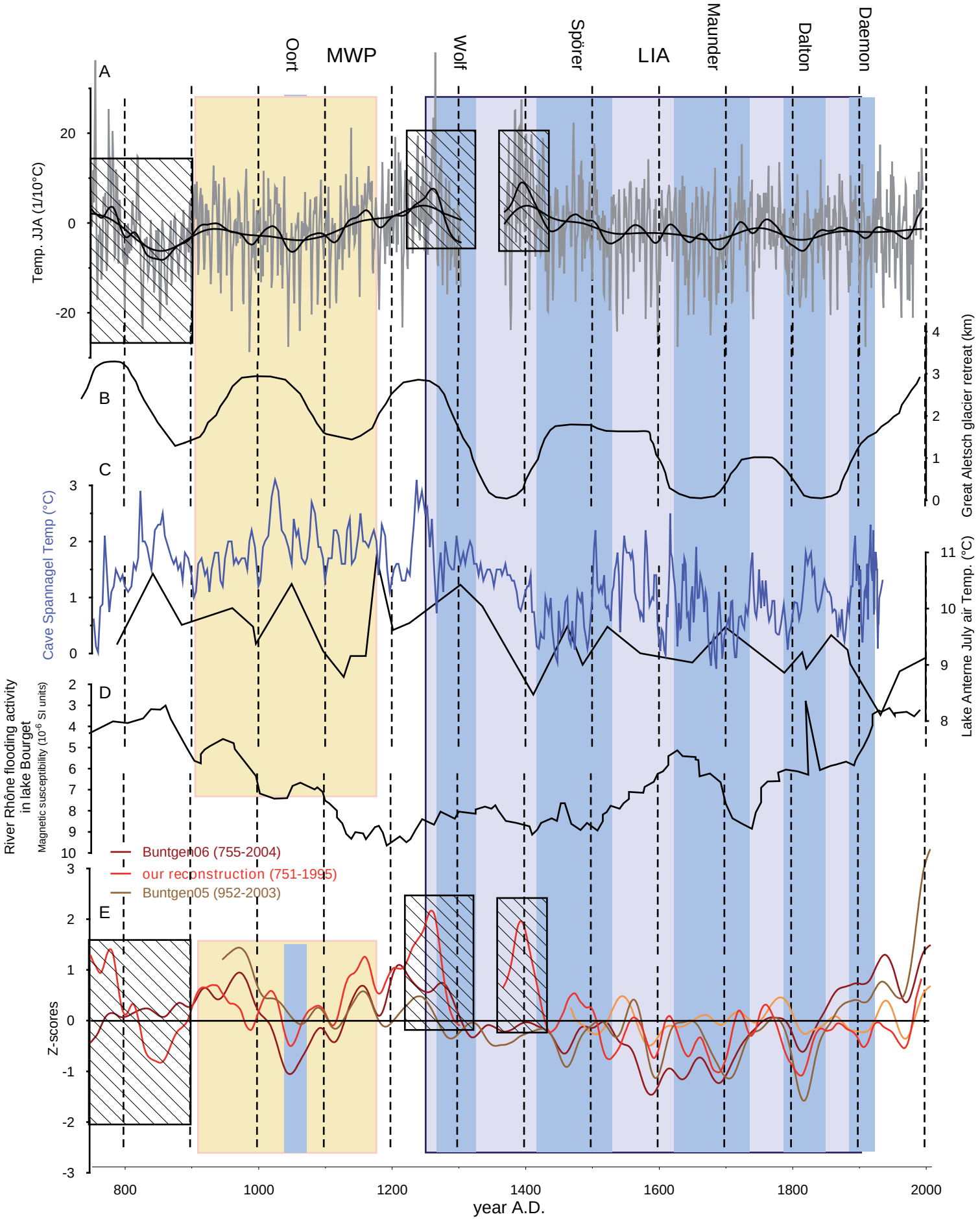
Oort
MWP
Wolf
Spörer
LIA
Maunder
Dalton
Daemon
A
B
C
D
E
Temp. JJA (1/10°C)
Great Aletsch glacier retreat (km)
Cave Spannagel Temp (°C)
Lake Anterne July air Temp. (°C)
River Rhône flooding activity in lake Bourget
Magnetic susceptibility (10⁻⁶ SI units)
Buntgen06 (755-2004)
our reconstruction (751-1995)
Buntgen05 (952-2003)
Z-scores
year A.D.